

## Supporting information

# Morphological and chemical transformations of single silica-coated CdSe/CdS nanorods upon fs-laser excitation

Wiebke Albrecht<sup>†\*</sup>, Bart Goris<sup>‡</sup>, Sara Bals<sup>‡</sup>, Eline M. Hutter<sup>¶</sup>, Daniel Vanmaekelbergh<sup>¶</sup>, Marijn A. van Huis<sup>†</sup>, and Alfons van Blaaderen<sup>†\*</sup>

<sup>†</sup>Soft Condensed Matter, Debye Institute for Nanomaterials Science, Utrecht University, Princetonplein 5, 3584 CC Utrecht, The Netherlands

<sup>‡</sup>Electron Microscopy for Materials Science (EMAT), University of Antwerp, Groenenborgerlaan 171, 2020 Antwerp, Belgium

<sup>¶</sup>Condensed Matter and Interfaces, Debye Institute for Nanomaterials Science, Utrecht University, Princetonplein 5, 3584 CC Utrecht, The Netherlands

\*To whom correspondence should be addressed.

E-mail: W.Albrecht@uu.nl; A.vanBlaaderen@uu.nl

## Methods

The 3.2 nm sized CdSe seeds were synthesized according to the hot injection method<sup>1</sup>. The CdSe/CdS NRs were then grown following a seeded growth approach which yielded 46 nm long and 5 nm thick NRs<sup>1,2</sup>. The CdSe/CdS NRs were coated with about 10 nm of silica according to the method described by Hutter et al.<sup>3</sup>. The reverse microemulsions were prepared by dispersion of 1.3 mL IgePAL CO-520 (NP-5) in 10 mL cyclohexane, followed by the addition of 1.6 nmol NRs in toluene and afterwards 80  $\mu$ L tetraethyl orthosilicate (TEOS). The solutions were continually stirred between these additions and there were at least 15 min between all additions. Finally, 150  $\mu$ L ammonia solution (10-12 wt%) was added after which the solution was stirred for one minute and then stored. The reaction was quenched one week after preparation of the microemulsion by addition of ethanol. The samples were then stored in ethanol. From TEM images we measured the average length and width of the CdSe/CdS NRs within the silica shells and found that they slightly decreased to 42 nm  $\pm$  7 nm and 4.5 nm  $\pm$  0.8 nm, respectively, which is in agreement with previous studies<sup>4</sup>. Two batches of silica-coatings were prepared under these conditions with the same CdSe/CdS NRs. Batch 1 was used for the experiments in Figure 1, 2, 3, S2, S3 and S7. Batch 2 was used for the experiments in Figure 4, 5, S4, S5, S6 and S8. Some CdSe/CdS NRs were slightly sticking out of the silica shells in the case of batch 2. This enabled us to compare completely and not completely covered NRs as discussed in Figure S4 and 4. The results for fully covered NRs were the same for both batches.

For the two-photon excitation experiments a Leica SP8 confocal setup (63x/1.32 NA oil-immersion confocal Leica objective) with an integrated Coherent chameleon II Ti:Sapphire laser (80 MHz repetition rate, about 140 fs pulse length) was used. In order to image the same particles before and after laser excitation a drop of the particle dispersion was dropcasted on formvar-coated TEM finder grids (Agar Scientific G2761) which were stabilized with an evaporated carbon film. TEM images of all particles in a spot of about 12  $\mu$ m  $\times$  12  $\mu$ m were taken by a TECNAI12 electron microscope before laser excitation (as shown in e.g. the upper row of Figure 2a). The grid was then sandwiched with a drop of glycerol between a microscopy glass slide and a 0.1 mm thick cover glass. Glycerol was chosen as its refractive index is close to silica, immersion oil and microscopy glass and could be easily removed (see below for procedure) from the TEM grid after illumination. By using the fiber-based white light laser of the SP8 confocal setup in reflection mode the spot looked at by TEM could be found back and brought into the focal plane. Subsequently, a thin 3D stack with about 12  $\mu$ m  $\times$  12  $\mu$ m 2D planes was scanned by the Ti:Sapphire laser (pixel size of 22.6 nm  $\times$  22.6 nm and pixel dwell time of 1.2  $\mu$ s). This was done since the focal plane can slightly change when switching between the two lasers. The excitation wavelength was 920 nm as the first absorption peak of the CdSe/CdS NRs lies at 460 nm (Figure 1). Taking the thin 3D stack took about 20 s which are about 64 frames for a pixel dwell time of 1.2  $\mu$ s. Assuming that

one particle spreads over 2 pixels and that every 12.5 ns a fs-laser pulse is delivered it can be estimated that the NRs absorbed about  $1.2 \cdot 10^4$  pulses. After removing the glycerol from the TEM grid by drying it overnight in vacuum the same particles were imaged by TEM again. The procedure was repeated for several spots to change the excitation fluence. The pulse fluence was calculated from the measured time-average laser power (using a Thorlabs PM200 powermeter with a S170C microscope slide power sensor) and the simulated point spread functions for this specific setup as shown in Figure 1. The point spread functions were simulated with the Huygens software version 15.10.1 for an excitation wavelength of 920 nm, a 63x/1.32 NA oil-immersion objective and glycerol as surrounding medium. For calculating the pulse fluence the pulse energy  $E_{peak}$  (average measured power divided by the repetition rate of the laser) was divided by the focal spot area ( $\pi \cdot r^2$  with r from Figure S1).

The EDX and high-resolution STEM (Figure 2b, 3 and 5) measurements were performed on an aberration-corrected microscope (FEI Titan G3) operated at 120 kV. The EDX maps were taken with the Esprit software by Bruker. The maps were acquired for 306 s (Figure 3a), 210 s (Figure 3b) and 90 s (Figure 5b) with a pixel size of 354 pm and a pixel dwell time of 18  $\mu$ s. The acquisition time of the EDX maps was kept short to avoid electron-beam induced transformations of the particles. Only EDX maps were included in the manuscript where the particles did not change during EDX acquisition. The EDX maps that are displayed in the manuscript and SI are intensity maps. In order to quantify the Cd:S ratio we extracted the spectrum corresponding to a whole particle or fragment and quantified it using the Cliff-Lorimer method. Only Cd and S were included in the quantification and the other elements were used for deconvolution only. It needs to be noted that the errors for quantification are relatively large due to the short acquisition time (about 15% for Cd and 8% for S). For the silica-coated NRs before deformation we obtained an average Cd:S ratio of 54:46. One example of an EDX intensity map of undeformed NRs is shown in Figure S8.

In-situ heating experiments were performed on a FEI Talos F200X operated at 200 kV using a heating holder from DENSSolutions. The NRs were dropcasted on a heating chip and inserted into the microscope. The temperature was increased in 50 °C steps and kept for 5 min at 50 °C, 100 °C, 150 °C, 200 °C, 250 °C, 350 °C, 400 °C and 550 °C, for 12 min at 300 °C, 33 min at 450 °C, 35 min at 500 °C, 8 min at 600 °C and 10 min at 700 °C.

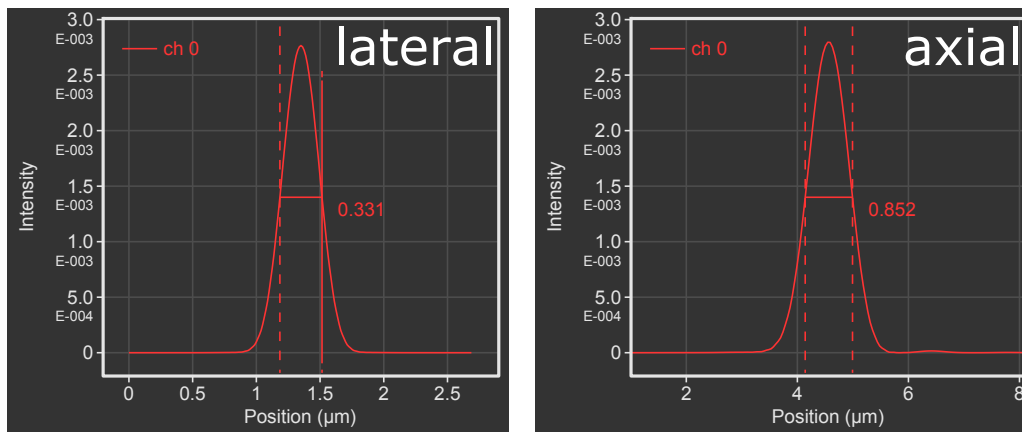


Figure S1: Lateral and axial profile with their FWHM of the simulated point spread functions for the used confocal setting. The FWHM of the lateral profile determines the radius r of the spot size and was used for calculating the fluences.

## Silica-coated NRs before and after fs-laser excitation

Figure S2 shows TEM images before and after fs-laser excitation (S2a) and a STEM image (S2b) of NRs that deformed into 1 (blue arrow) or 3 fragments (red arrows).

A few NRs showed bright spots on the surface before laser illumination as presented in Figure S3 (e.g. marked by the white arrows). High-resolution STEM or EDX measurements could not be performed due to the beam sensitivity of the particles. Thus, it could not be confirmed if the observed spots as shown in Figure S3 are Cd. Furthermore, it is not clear whether these were already present or formed by the electron beam. It could be that excess Cd atoms from the synthesis form very small aggregates under the electron beam.

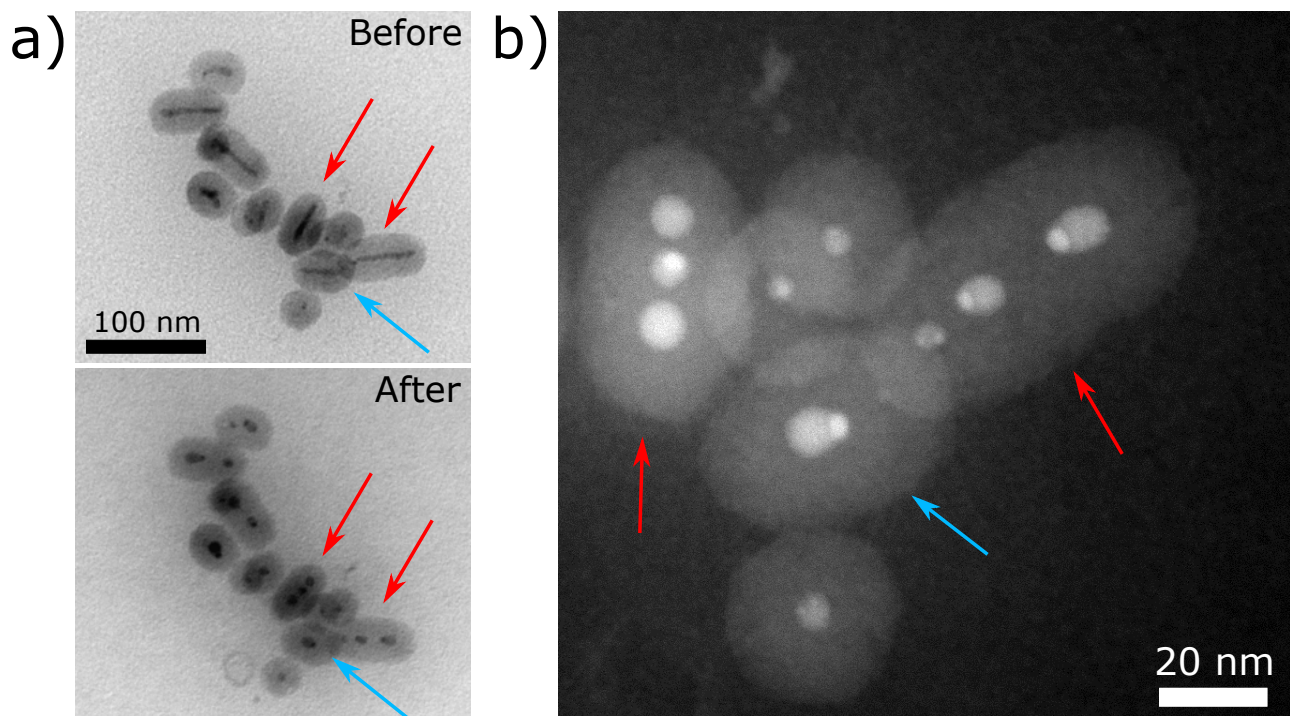


Figure S2: a) TEM images before and after excitation of fs-laser pulses with a pulse fluence of  $5.8 \text{ mJ/cm}^2$ . The blue arrows mark spot where only one fragment was observed after laser illumination. The red arrows mark NRs that deformed into 3 fragments. b) HAADF-STEM close-up of the marked particles in a.

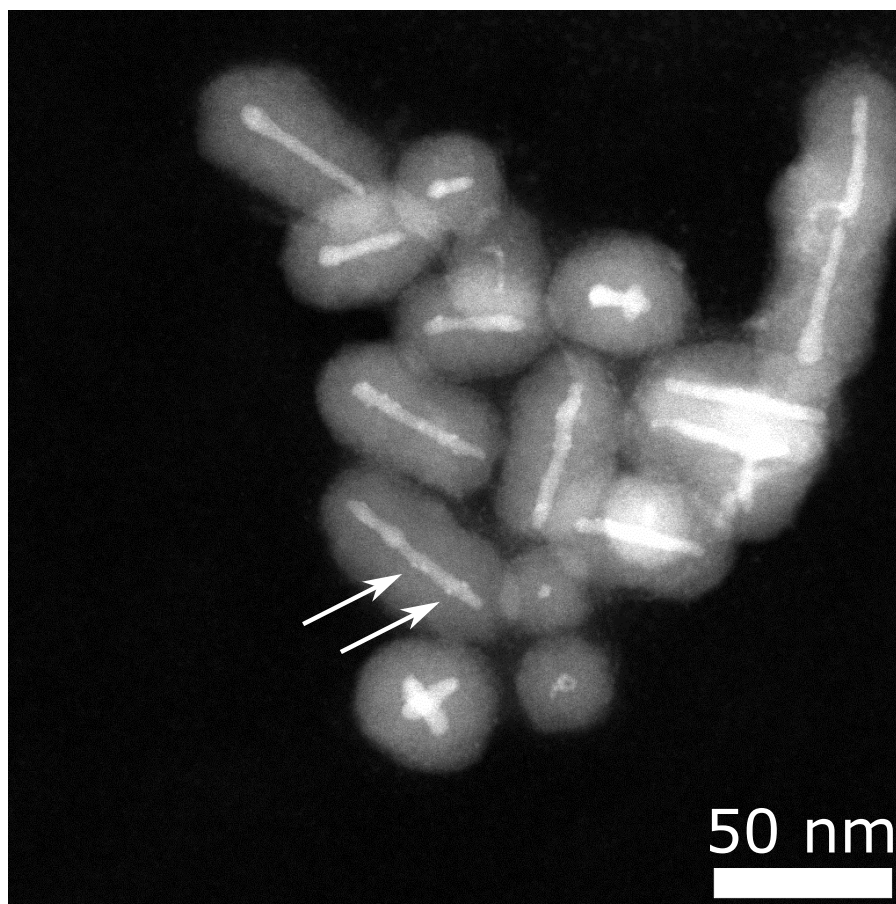


Figure S3: HAADF-STEM image of undeformed silica-coated CdSe/CdS NRs exhibiting small white spots which could be tiny Cd aggregates formed from excess Cd atoms from the synthesis.

## Impact on uncoated and not fully covered NRs

Figure S4a shows TEM images of uncoated CdSe/CdS NRs before and after illumination with 2.6 mJ/cm<sup>2</sup> fs-laser pulses. The NRs were from the same batch that was used for all other experiments. All particles sublimated and thus it can be concluded that the silica shell stabilizes the particles. Figure S4b presents TEM images of silica-coated CdSe/CdS NRs before and after fs-laser illumination with a pulse fluence of 7 mJ/cm<sup>2</sup>. It can be seen that particles that were not fully covered by the silica shell (marked by arrows) partially or completely sublimated without deformation, most likely through the hole in the silica shell where the particle was sticking out, whereas the fully covered NRs deformed into spherical fragments.

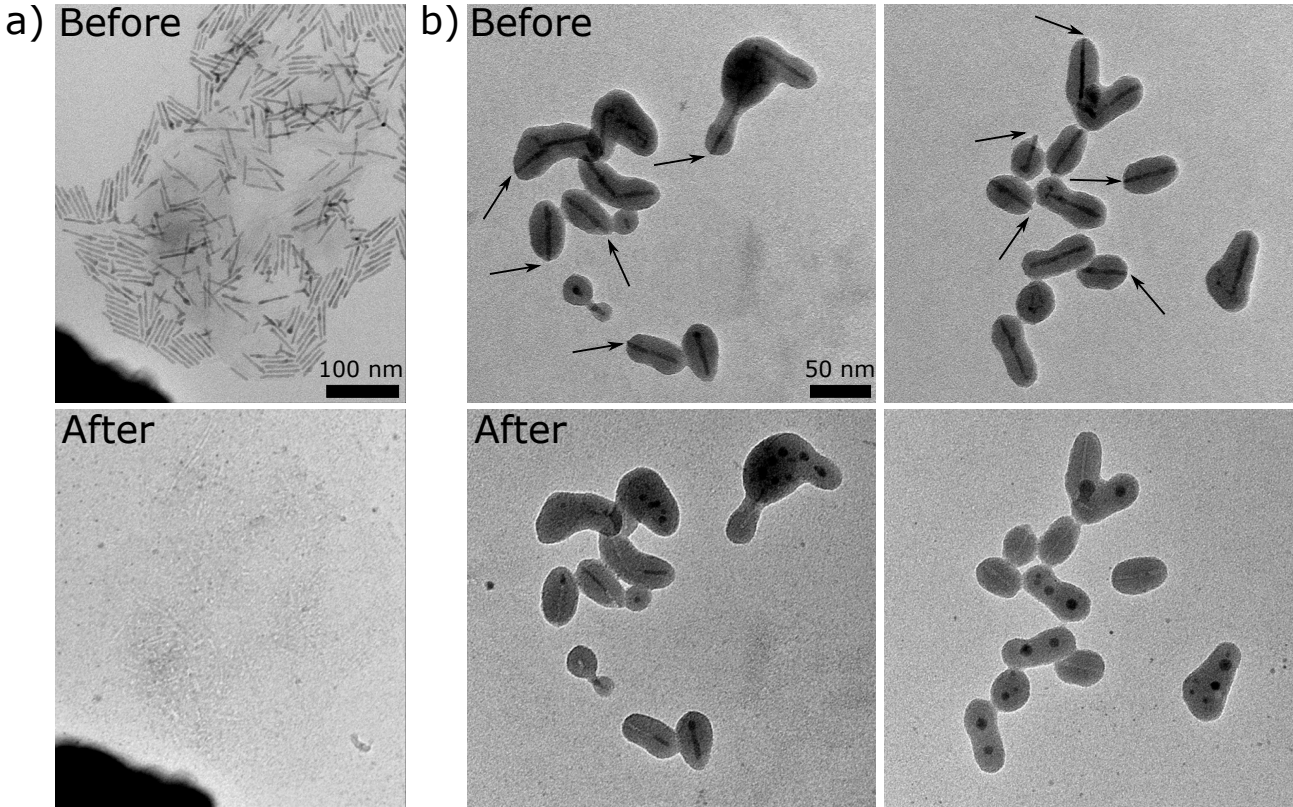


Figure S4: a) TEM images of uncoated CdSe/CdS NRs before and after illumination with 2.6 mJ/cm<sup>2</sup> pulses. b) TEM images of fully and not fully covered silica-coated CdSe/CdS NRs before and after illumination with 7 mJ/cm<sup>2</sup> pulses.

## Lattice spacings of CdS and Cd

The lattice spacings were obtained by measuring the distances of two reflections in the diffractograms (Figure 2c). The distances were measured 10 times and then averaged. Wurtzite CdS has the two lattice constants  $a=0.4160$  nm and  $c=0.6756$  nm. The lattice constants of hexagonal close-packed Cd are  $a=0.2979$  nm and  $c=0.5619$  nm. For hexagonal lattices the lattice spacings  $d_{hkl}$  can then be calculated by the following equation:

$$\frac{1}{d_{hkl}^2} = \frac{4}{3} \left( \frac{h^2 + hk + k^2}{a^2} \right) + \frac{l^2}{c^2} \quad (1)$$

The obtained values are discussed in the main text.

## Electron beam influence

The fragments formed after fs-laser illumination sometimes changed under the electron beam. For example, Cd spots 'grew' or dissolved within the CdS lattice under electron beam exposure. An example is shown in Figure S5. The three fragments did not show a Cd segregated spot after laser illumination but under the electron beam such spots grew in the case of all fragments (Figure S5a). After zooming in on the upper fragment the just created spots dissolved again (Figure S5b).

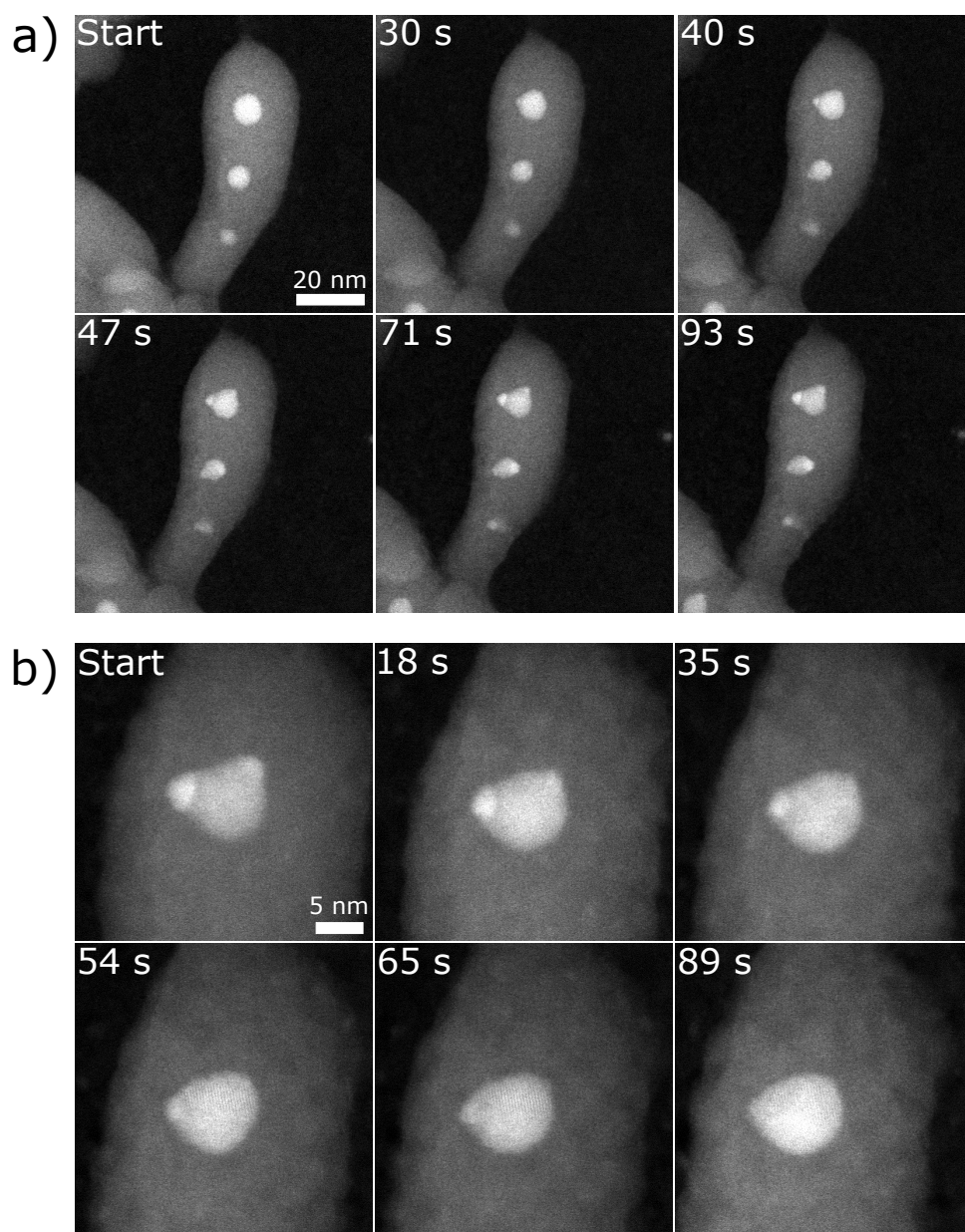


Figure S5: a) Stills of a HAADF-STEM recording showing electron beam induced growth of segregated Cd spots at NR fragments that were created after fs-laser excitation. b) Dissolution of the just created spots after zooming in.

Figure S6 shows the continuation of the movie in Figure 5 after zooming in to the upper fragment. The Cd spot continued to grow at the expense of the CdS lattice until there was no CdS left.

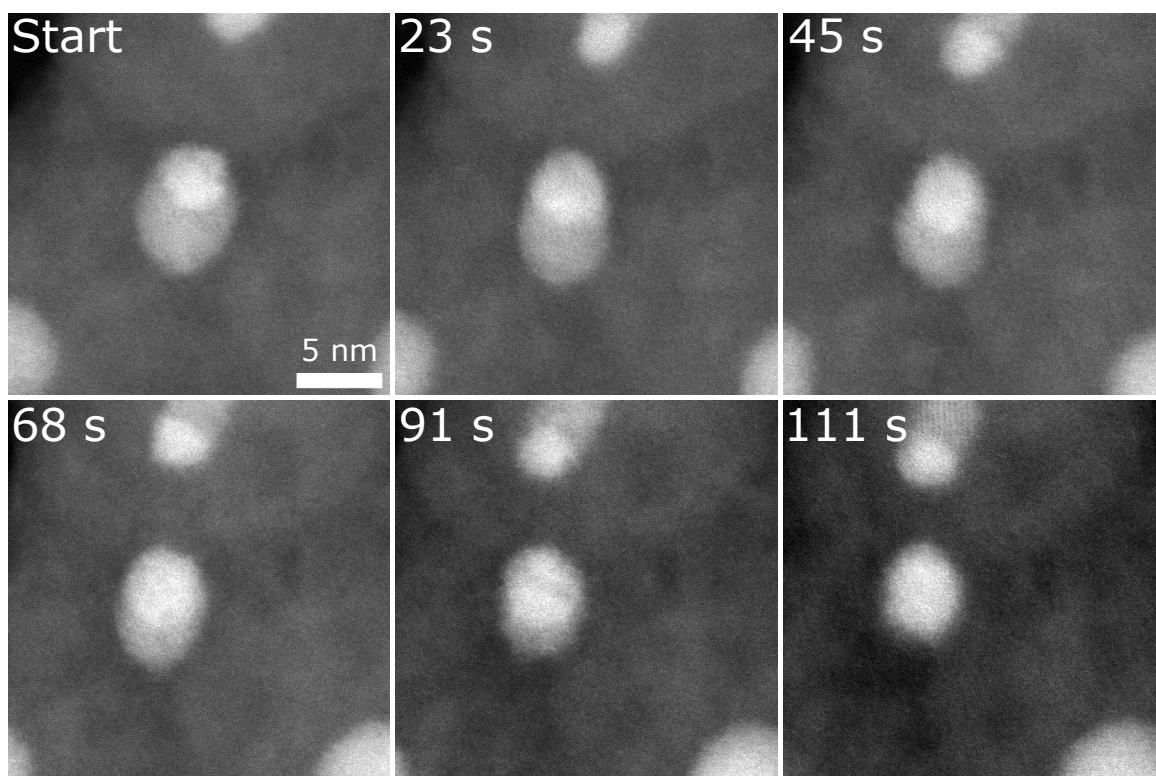


Figure S6: Continuation of the series of STEM images from Figure 5 in the main text. A zoomed-in new movie was started. The elapsed time of this second movie is denoted in the STEM images.

### Additional EDX maps

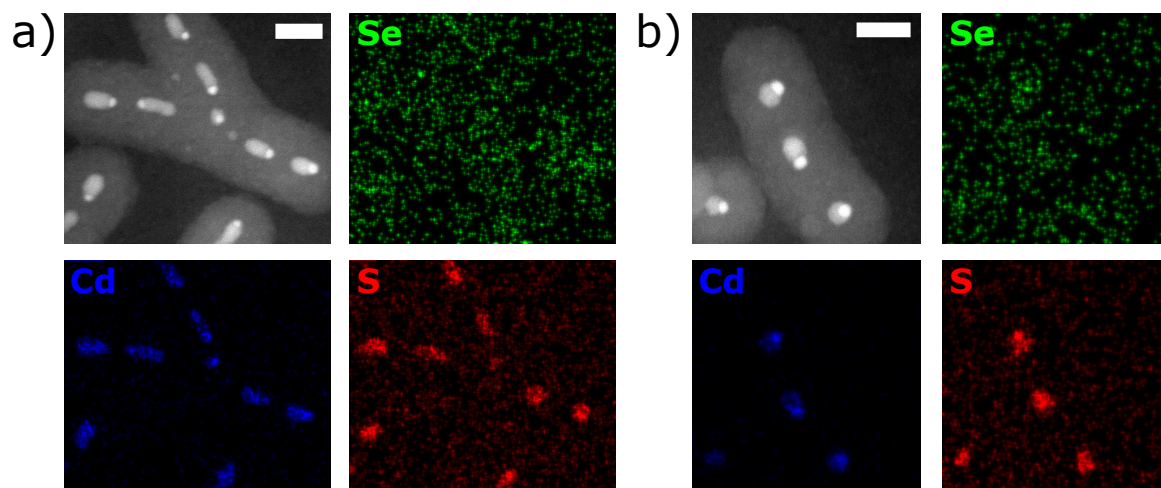


Figure S7: EDX intensity maps from a) Figure 3a and b) Figure 3b including Se maps. The CdSe core could not be mapped due to its small size of about 3 nm. The scale bars represent 20 nm.

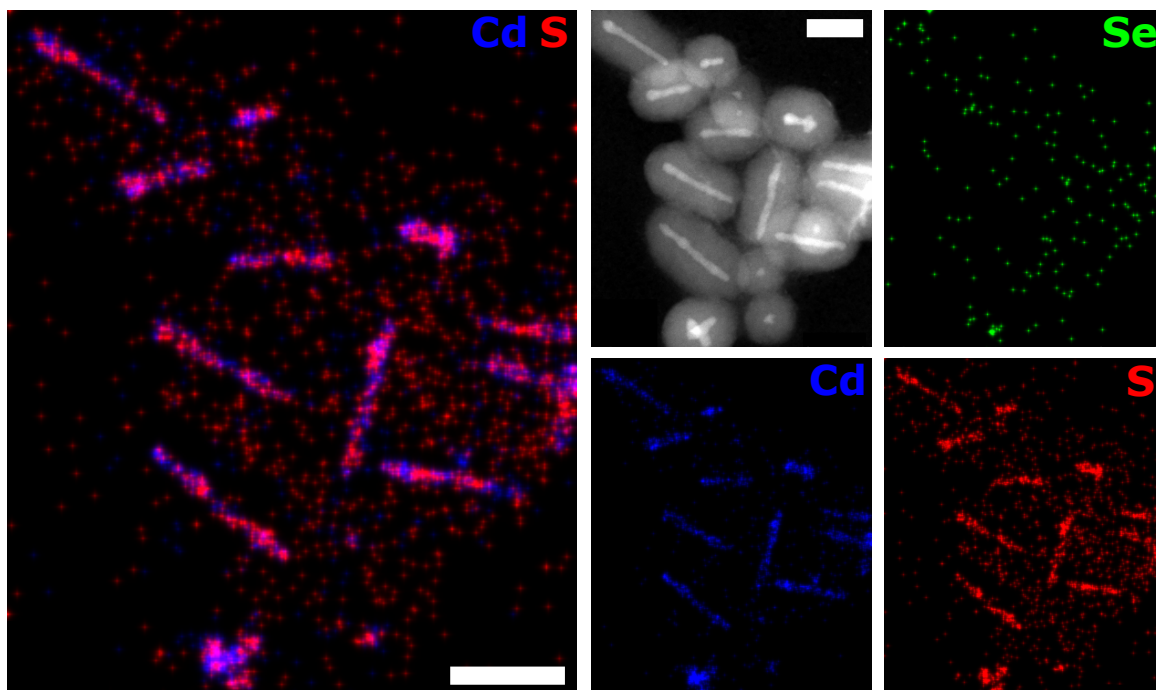


Figure S8: EDX intensity maps of silica-coated undeformed CdSe/CdS NRs. The map was acquired for 236 s with a pixel dwell time of 23  $\mu$ s. By quantification of the Cd and S counts we determined a Cd:S ratio of 51:49 for the displayed map. By quantifying a total of six similar maps of silica-coated undeformed NRs we obtained an average Cd:S ratio of 54:46. The scale bars represent 30 nm.

## References

- [1] Carbone, L. et al. *Nano Lett.* **2007**, *7*, 2942–2950.
- [2] Pietra, F.; van Dijk - Moes, R. J. A.; Ke, X.; Bals, S.; Van Tendeloo, G.; de Mello Donega, C.; Vanmaekelbergh, D. *Chem. Mater.* **2013**, *25*, 3427–3434.
- [3] Hutter, E. M.; Pietra, F.; Van Dijk - Moes, R. J. A.; Mitoraj, D.; Meeldijk, J. D.; De Mello Donegá, C.; Vanmaekelbergh, D. *Chem. Mater.* **2014**, *26*, 1905–1911.
- [4] Anderson, B. D.; Wu, W.-C.; Tracy, J. B. *Chem. Mater.* **2016**, *28*, 4945–4952.